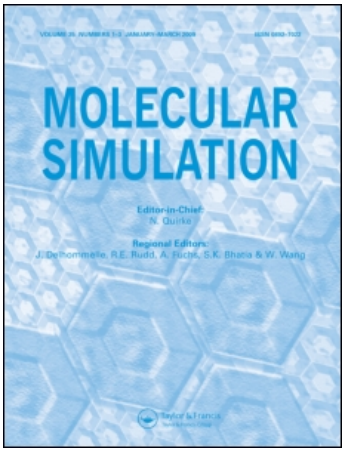

Molecular Simulation
Publication details, including instructions for authors and subscription information:
http://www.informaworld.com/smpp/title~content=t713644482

An Application of Classical Molecular Dynamics Simulation and AB Initio Density-Functional Calculation in Surface Physics

H. Rafii-Tabar[a]; H. Kamiyama[a]; Y. Maruyama[a]; K. Ohno[a]; Y. Kawazoe[a]
[a] Institute for Materials Research, Tohoku University, Aoba-ku, Sendai, Japan

To cite this Article Rafii-Tabar, H. , Kamiyama, H. , Maruyama, Y. , Ohno, K. and Kawazoe, Y.(1994) 'An Application of Classical Molecular Dynamics Simulation and AB Initio Density-Functional Calculation in Surface Physics', Molecular Simulation, 12: 3, 271 — 289
To link to this Article: DOI: 10.1080/08927029408023036
URL: http://dx.doi.org/10.1080/08927029408023036

Molecular Simulation, 1994, Vol. 12(3-6), pp. 271-289
Reprints available directly from the publisher
Photocopying permitted by license only

AN APPLICATION OF CLASSICAL MOLECULAR DYNAMICS SIMULATION AND AB INITIO DENSITY-FUNCTIONAL CALCULATION IN SURFACE PHYSICS

H. RAFII-TABAR, H. KAMIYAMA, Y. MARUYAMA, K. OHNO and Y. KAWAZOE

Institute for Materials Research, Tohoku University, 2-1-1 Katahira, Aoba-ku, Sendai 980, Japan

(Received March 1993, accepted May 1993)

Classical molecular dynamics simulation and ab initio mixed basis Car-Parrinello methods are discussed and applied to the investigation of the results of a recently performed STM-based experiment involving the adsorption of C_{60} molecules on the dimerized Si surface. We show that these methods are capable of providing the theoretical basis for this experiment and test the validity of the associated conjectures.

A mixed-basis all-electron formalism for the Car-Parrinello method is proposed to obtain the detailed understanding of the electronic states and dynamics of surface structure. A band structure calculation using this formalism is performed for the $c(4 \times 3)$ structure of C_{60} adsorbed on Si (100) surface and is compared with the experimental results.

KEY WORDS: Classical MD simulations, Car-Parrinello method, mixed-basis DFT, C_{60} Buckyballs, Si(100) $c(2 \times 1)$ surface, Tersoff potential

1 INTRODUCTION

Computer-based Molecular Dynamics (MD) simulations have now become standard methodologies for investigating, at the atomistic and molecular levels, theoretical and experimental problems in condensed matter physics and materials science. Employing these methods, we are now able to understand the collective behaviour and properties of complex systems and their emergent properties in condensed phase in terms of motions of their individual constituents, and to predict their time evolutions under controlled conditions. In materials science, MD simulations have been employed over the past few years to provide insights into the processes that emerge in stressed nano-volumes of solids in order to elucidate the atomistic mechanisms underlying the macroscopic processes of plasticflow, adhesion, sintering, indentation, fracture, friction and dislocation nucleation in metals [1, 2, 3].

Recently, problems in surface physics of metals and semi-conductors have provided the fertile grounds for further applications of MD simulations in materials science. The adsorptions of monolayers and multilayers of molecules and micro- and nano-clusters on metallic and semi-conducting surfaces can now be simulated to provide insights into the corresponding STM-based, and other, experimental investigations performed in this field.

A classical MD simulation proceeds by considering a finite nano-size cluster of

atoms, the size of which depends on the computational power available, in a primary computational cell that is periodically replicated in three dimensions. These replicated image cells, containing the periodic images of the atoms in the central cell, form the periodic boundary conditions that are introduced to minimise the effects of the artificial surfaces that arise due to the finite size of the nano-clusters considered. Methods are now available for constructing computational cells pertinent to atomic configurations with the BCC, FCC and HCP structures.

In an MD simulation, the energetics and dynamics of the system are derived from inter-atomic potentials of pairwise-additive and, more recently, of many-body types. These include Lennard-Jones potentials, appropriate for the description of closed-shell materials, Stillinger-Weber Si potentials [4], Finnis-Sinclair many-body pure metallic [5] and alloy [6] potentials, Embedded-Atom many-body metallic [7] and Si [8] potentials and non-central many-body Tersoff potentials [9] for covalently-bonded systems of C and Si atoms.

Each atom within the computational cell interacts with a set of neighbours that lie within the cut-off radius of the potential. Powerful procedures now exist [10] for constructing and updating atomic neighbour lists. The forces that are experienced by the atoms are obtained from these potentials, and the numerical integration of the resulting differential equations of motion via finite-difference techniques, such the Verlet algorithms [11], the Gear Predictor-Corrector algorithms [12], is employed to provide the atomic world lines within the computational cell.

The classical MD simulation that will be reported in this paper is of the equilibrium type applied to a canonical ensemble in which the number of atoms and the volume of the computational cell are both fixed, and the temperature of the system is maintained at a constant preset value. We report in this paper the results of our classical MD simulation of monolayer adsorption of C_{60} Buckyballs on the Si(100) $c(2 \times 1)$ reconstructed surface. Our simulation, performed on a relatively small system, is capable of shedding light on the experimental results that have recently been obtained for this system.

Band structure calculation is one of the most important methods for investigating the electronic structure of materials. Local density approximation in density functional theory together with pseudopotentials and plane wave expansions of wave functions are convenient methods to calculate electronic states of materials. Although recent advances in computational power have made it possible to increase the number of basis sets in the expansion of wave functions, resulting in more precise electronic structure calculations, it is rather difficult to deal with light elements such as carbon, boron and nitrogen because the strong Coulomb potential near the nuclei can hardly be removed from the pseudopotentials. Typically 32,000 ~ 45,000 plane waves [28] (about 35Ryd to 45Ryd in energy cutoff) are required for simulating the correct bond lengths of small carbon clusters like C_{10} in a pseudopotential formalism. In such a case, the use of pseudopotentials does not reduce the total amount of the calculation. Hence for light atoms, the full-potential calculation in dealing with all core electrons as well as all valence electrons is the next desired step towards a more precise analysis.

In this paper, we introduce a new method for performing an *ab-initio* molecular dynamics simulation for the full-potential and all-electron calculation in the *mixed-basis approach* which uses both Plane Waves (PW) and the 1s core- and 2p valence-

atomic orbitals (AOs). We will apply this method to the C_{60} molecule residing on the Si(100) surface.

2 THE C_{60}/SI SYSTEM

Considerable scientific and technological interests have been generated during the past few years over the study of C_{60} Fullerenes (Buckyballs) as novel forms of carbon in condensed phase laying in the range between the small carbon molecules and the bulk phase. In particular, it has been established [13, 14] that the doping of the C_{60} crystals with alkali metal atoms leads to superconducting compounds with transition temperatures in excess of 30 K. Both experimental investigations [15, 16] and theoretical studies [17–20] concerning the structure and properties of this molecule have confirmed its truncated icosahedral soccer-ball geometry having an unusual degree of stability. Moreover, it is now known that the solid C_{60} crystal is an FCC structure, with a centre-to-centre distance of 10.02 Å, in which the molecules undergo rotational diffusion under ambient conditions [15, 16].

Another field of investigation involving the C_{60} Buckyballs has been the studies of C_{60} overlayer growth on metallic and semi-conductor surfaces using Scanning Tunnelling Microscopy (STM). Employing the STM, it has been established [21, 22] that the C_{60}s deposited on the Au(111) surface display mobile hexagonal arrays with an inter-molecular spacing of 11.0 Å, while those adsorbed on the GaAs surface [23, 24] reveal large locally-ordered first monolayer islands that are structurally stable and commensurate with the underlying substrate.

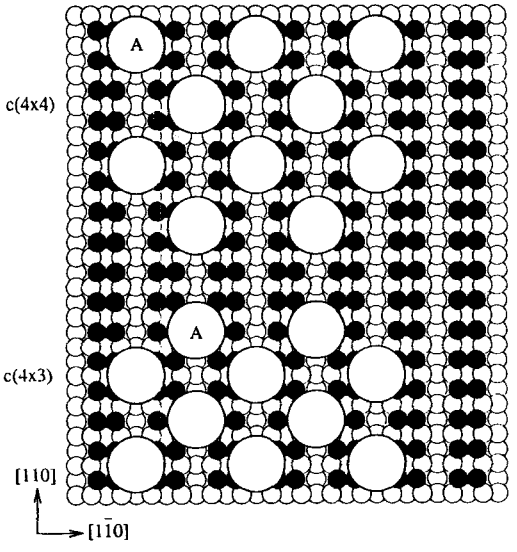

Figure 1 Schematic positions of the C_{60} molecules on the Si(100) c(2 × 1) surface: (a) c(4 × 3) forming the hexagonal arrays, and (b) c(4 × 4) forming the simple cubic arrays. (Open circles are bulk positions of Si atoms, solid circles are dimerized surface Si atoms, and large open circles indicate the positions of C_{60} molecules). Figure reproduced from Ref. 25.

Very recently the first field ion STM-based results [25] of monolayer and multilayer depositions of C_{60} molecules on Si(100) c(2 × 1) reconstructed surface have been reported. In contrast to the Au and GaAs surfaces, the Si dimerized substrate is an "active" surface with each Si atom contributing a dangling bond, and hence it is expected that there would be a significant amount of charge transfer to the deposited C_{60} molecules. On the basis of a large number of STM scans, the following conjectures were proposed:

(a) The absorbed C_{60} molecules reside in the troughs of the dimer rows on the surface and are distributed randomly with a minimum separation of 12 Å.

(b) The individual molecules occupy site A in Figure 1 with a high degree of symmetry and are surrounded by eight dimer-forming Si atoms. This figure was produced in Ref. [25] on the basis of an STM image of a coverage of approximately 0.02 C_{60} monolayer.

(c) There appears to be no coalescence on the terraces or no segregation to the steps or the defects at room temperature, unlike the case of C_{60}s adsorbed on GaAs(110) surface.

(d) There is only a short-range local ordering of the C_{60}s the first deposited layer. There are two types of structures observed: c(4 × 3) and c(4 × 4) as seen in the STM image in Figure 2. The c(4 × 3) lattice forms the FCC(111) plane as well as the HCP basal plane and the c(4 × 4) forms the simple cubic(001) plane. The nearest-neighbour distances are 9.6 Å and 10.9 Å for the c(3 × 4) and c(4 × 4) respectively. With the completion of

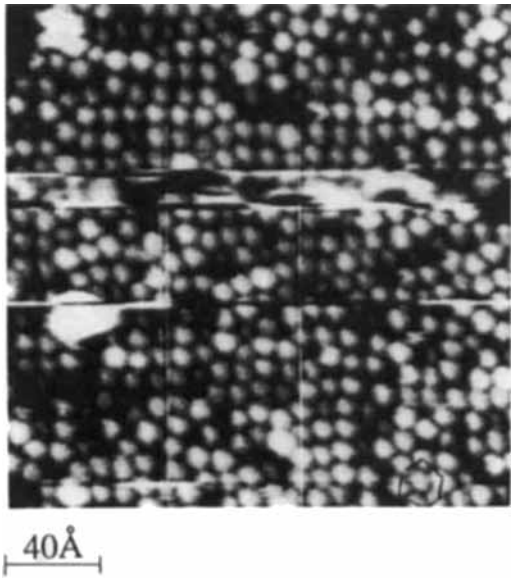

Figure 2 STM image of the surface with the C_{60} coverage of approximately one monolayer, showing both the c(3 × 4) and c(4 × 4) packings. The dark regions are still unfilled bare Si surface. Figure reproduced from Ref. 25.

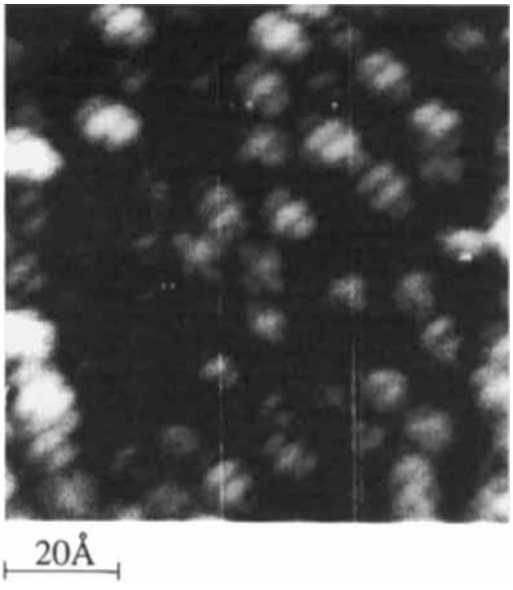

Figure 3 STM image of the first layer of the C_{60} molecules. The image shows some internal structure (three or four rows running in parallel) for the individual C_{60} molecules. Similar internal structures were also observed for the C_{60} adsorbed on the Si(111) c(7 × 7) surface. Figure reproduced from Ref. 25.

the first layer, the second layer of C_{60}s begins to form and island formation is also observed suggesting a Stranski-Krastanov growth mode.

(e) There are STM images that show some structure on individual C_{60} molecules. In Figure 3 three or four bright rows run in parallel on each molecule. Since the orientations of these "stripes" are the same, this could indicate that the Buckyballs are not rotating on the Si(100) surface at room temperature. The origins of these stripes may be attributed to the transfer of charges from the dangling bonds to the molecules.

To give a theoretical insight into the dynamics of single and collective interactions of C_{60} molecules with the Si(100) dimerized surface and examine the validity of the above conclusions, we have performed an ab initio density-functional calculation and a large-scale classical MD simulation modelling as closely as possible the experimental procedure for monolayer deposition on a substrate. We have found that our results are in close agreement with most of the above experimental findings.

3 CLASSICAL MOLECULAR DYNAMICS SIMULATIONS

The inter-atomic potentials that we have used to describe the interactions between the Si atoms in the substrate and between the Si atoms and the C atoms on the Buckyballs are Tersoff non-central many-body potentials [9]. These potentials represent the current state of the art in describing the cohesive energies of covalently-bonded Si and C solids. According to these potentials, the total energy

of a system of atoms is modelled as a sum of pair interactions with the coefficient of the attractive component in the pairwise potential (which plays the role of a bond order) depending on the local atomic environment and hence giving rise to many-body contributions. The energy E, as a function of the atomic coordinates, is taken to be:

$$E = \sum_i E_i = \frac{1}{2} \sum_{i \neq j} V_{ij}, \quad V_{ij} = f_c(r_{ij}) \left[f_R(r_{ij}) + b_{ij} f_A(r_{ij}) \right];$$

$$f_R(r_{ij}) = A_{ij} \exp(-\lambda_{ij} r_{ij}), \quad f_A(r_{ij}) = -B_{ij} \exp(-\mu_{ij} r_{ij});$$

$$f_c(r_{ij}) = \begin{cases} 1, & r_{ij} < R_{ij} \\ \frac{1}{2} + \frac{1}{2} \cos\left[\pi (r_{ij} - R_{ij}) / (S_{ij} - R_{ij}) \right], & R_{ij} < r_{ij} < S_{ij}, \\ 0, & r_{ij} > S_{ij}; \end{cases}$$

$$b_{ij} = \chi_{ij} (1 + \beta_i^{n_i} \zeta_{ij}^{n_i})^{-1/2n_i}, \quad \zeta_{ij} = \sum_{k \neq i,j} f_c(r_{ik}) \omega_{ik} g(\theta_{ijk}),$$

$$g(\theta_{ijk}) = 1 + c_i^2/d_i^2 - c_i^2/[d_i^2 + (h_i - \cos\theta_{ijk})^2];$$

$$\lambda_{ij} = (\lambda_i + \lambda_j)/2, \quad \mu_{ij} = (\mu_i + \mu_j)/2, \quad \omega_{ik} = \exp[\mu_{ik}^3 (r_{ij} - r_{ik})^3],$$

$$A_{ij} = (A_i A_j)^{1/2}, \quad B_{ij} = (B_i B_j)^{1/2}, \quad R_{ij} = (R_i R_j)^{1/2}, \quad S_{ij} = (S_i S_j)^{1/2},$$

where i, j, k label the atoms of the system, r_{ij} is the length of ij bond, and θ_{ijk} is the bond angle between ij and ik. Singly subscripted parameters, such as λ_i and n_i, depend only on the type of the atom (C, Si). The parameters of the potentials are given in Table 1.

The Buckyballs were treated as rigid molecules, with their atoms interacting via Lennard-Jones 12-6 potentials:

$$V(I, J) = 4\varepsilon \sum_{i,j} \left[\left(\frac{\sigma}{r_{ij}^{IJ}} \right)^{12} - \left(\frac{\sigma}{r_{ij}^{IJ}} \right)^{6} \right]$$

where I and J denote two molecules, r_{ij}^{IJ} is the distance between the atom i in

Table 1. Parameters of Tersoff potentials for C and Si.

	C	*Si*
$A(eV)$	1.3936×10^3	1.8308×10^3
$B(eV)$	3.467×10^2	4.7118×10^2
$\lambda(\text{Å}^{-1})$	3.4879	2.4799
$\mu(\text{Å}^{-1})$	2.2119	1.7322
β	1.5724×10^{-7}	1.1000×10^{-6}
n	7.2751×10^{-1}	7.8734×10^{-1}
c	3.8049×10^4	1.0039×10^5
d	4.384×10^0	1.6217×10^1
h	-5.7058×10^{-1}	-5.9825×10^{-1}
$R(\text{Å})$	1.8	2.7
$S(\text{Å})$	2.1	3.0

$\chi_{C-C} = \chi_{Si-Si} = 1$, $\chi_{C-Si} = 0.9776$

molecule I and atom j in molecule J with parameters ($\varepsilon = 28\,\mathrm{K}$ and $\sigma = 3.4\,\text{Å}$) taken from Ref. [26]. The classical equations of motions were integrated numerically via the velocity Verlet algorithm [27]. This procedure takes the form:

$$r(t + dt) = r(t) + dt \cdot v(t) + \frac{1}{2}(dt)^2 \cdot a(t)$$

$$v\left(t + \frac{1}{2}dt\right) = v(t) + \frac{1}{2}dt \cdot a(t)$$

$$v(t + dt) = v\left(t + \frac{1}{2}dt\right) + \frac{1}{2}dt \cdot a(t + dt)$$

and it is implemented in a simulation program by first calculating the positions of all atoms at time $t + dt$, and their velocities at mid-step $t + \frac{1}{2}dt$. The forces and accelerations at time $t + dt$ are then computed and these are used to update the velocities at $t + dt$. At this point, the kinetic energy is available at time $t + dt$. The method uses 9N words of storage (N is the number of atoms) and is numerically very stable.

The temperature of the system in our simulation was maintained at a fixed value by rescaling the particles' velocities at each time step. The energy relaxation during the equilibration phase was performed via a quenched MD algorithm in which the velocities of atoms were quenched to zero every time the total kinetic energy of the system reached its maximum value.

4 CLASSICAL MOLECULAR DYNAMICS RESULTS

Our MD simulation was performed for a Si substrate having 9 atomic layers with 128 atoms per layer. With the exception of the atoms in the lowermost layer, all

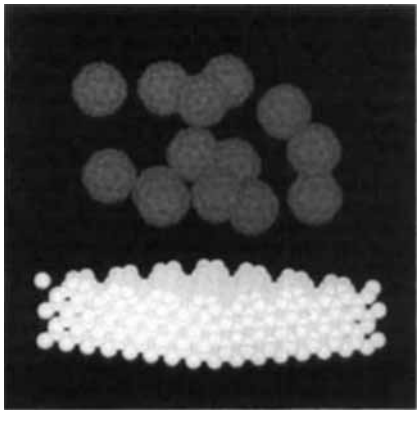

Figure 4 The initial configuration showing the randomly distributed Buckyballs above the Si(100) surface. Vertical direction is ⟨001⟩, horizontal direction is ⟨1$\bar{1}$1⟩, ⟨110⟩ direction is into the plane of the paper.

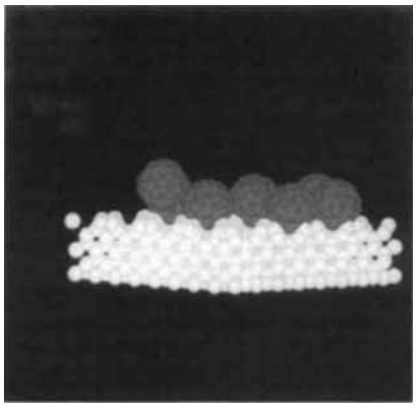

Figure 5 Final positions of the Buckyballs in the troughs of the dimer rows. Directions are the same as Figure 4.

other atoms were treated dynamically. Periodic boundary conditions were applied in all three directions. To mimic the experimental technique of film deposition, our initial configuration of Buckyballs, consisting of 14 molecules, was randomly distributed over the dimerized substrate in the direction of (001) normal to the surface as shown in Figure 4. An equilibration run of 1000 time steps ($dt = 10$ fs) at constant temperature of 300 K and constant pressure was then performed to relax the system. During this phase, we insured that there were no interactions between the Buckyballs and the substrate. Following the equilibration, the Buckyballs were released in the direction of the substrate with a kinetic energy corresponding to that of the room temperature. The animation of the complete run using three-dimensional computer-generated geometries shows that the Buckyballs continuously interact with one another as well as with the surface before they come to be captured by the substrate. Figure 5 shows that the C_{60}s do indeed end up and stay in the

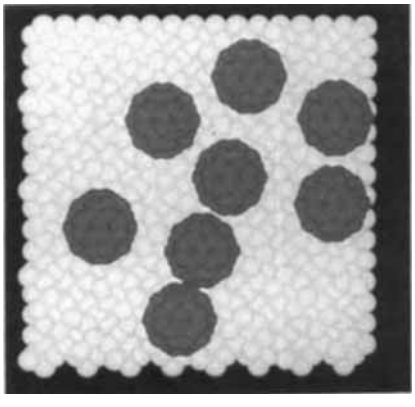

Figure 6 The alignments of the Buckyballs on the surface of Si showing the formation of c(4 × 4) structure. The horizontal direction is ⟨100⟩, and the vertical direction is ⟨010⟩.

dimer valleys and are surrounded by the eight dimer-forming Si atoms as predicted experimentally and displayed in Figure 1. Furthermore, we observe from Figure 6 the formation of the $c(4 \times 4)$ structure where we have removed, for convenience, those Buckyballs undergoing the periodic boundary conditions. This result is in agreement with conjecture (d) stated above, but in this simulation we did not observe the formation of $c(4 \times 3)$ structure. Furthermore, since the surface of the substrate in our simulation did not have any steps, or other defects, we did not study the question of segregation etc. We can summarize this part of our work by stating that our large-scale constant temperature classical MD simulation based on the interatomic potentials that were employed is capable of reproducing much of the experimental results and therefore offers an insight into the dynamics of the Buckyballs on the Si(100) surface.

We now turn to the *ab-initio* band structure calculations that we have carried out for the $C_{60}c(4 \times 3)$ thin film structure deposited on Si (100) surface.

5 MIXED-BASIS METHOD WITH CAR-PARINNELLO FORMALISM

The Car-Parrinello (CP) method [29] and the related simulated annealing approach of *ab-initio* molecular dynamics simulations, have been successfully applied to the investigation of electronic and atomic structures and vibrational modes of variety of systems. These approaches avoid any conventional matrix diagonalizations and deal with the updating of atomic positions and the calculation of electronic states simultaneously within the adiabatic approximation. The advantage of these approaches is that they require relatively small memory size and computational time. Besides the original CP method that begins with a classical Lagrangian, several variations have been proposed that treat the electronic dynamics differently; the steepest descent (SD) method, the conjugate gradient method and so forth, for rapid convergence of the electronic states [30, 31]. These approaches combined with the local density approximation [32], the pseudopotentials [33, 34] and the expansion in terms of plane waves (PWs) of the electronic states have been successfully applied to the covalent electron orbitals such as those in simple semiconductors like silicon [29].

Recently, however, several problems associated with these methods have been discussed in the literature [35]. The first problem occurs in the choice of pseudopotentials themselves. In the course of using the standard separable type of pseudopotentials [34], it has been pointed out that one should pay more attention to the unphysical features, e.g. the so-called ghost states. The use of more reliable pseudopotentials would require more PWs and hence more computational time. The second problem occurs in the treatment of the localized electron orbitals, (here as an another problem, the self-interaction correction [36] also becomes important in the density functional formalism [32]). In this case, again it would be necessary to use quite a large number of PWs to describe the localized orbitals and much longer computational time to achieve a good convergence of the expansion coefficients. Sometimes, to preserve the Born-Oppenheimer (BO) surface may be not so easy in the original CP approach which uses only PWs.

In the present paper we have extended the formalism, relying only upon the pseudopotentials and the PW expansion. Here, we concentrate our main interest on treating light atoms such as carbon, boron and nitrogen.

Historically the mixed-basis approach in the band structure calculation was first introduced by Friedli and Ashcroft [37] in the case of hydrogen molecular crystals, and a similar approach was applied to the case of transition metals by Louie, Ho and Cohen [38] in order to handle the spatial locality and asymmetry of the *d*-orbitals correctly. The present work is the first attempt to apply the mixed-basis to the *ab-initio* full-potential molecular dynamics simulation of a carbon micro-cluster [40, 41].

For the dynamics of electrons, we use the usual SD method having the first derivative with respect to t so as to keep the electronic states near the BO surface at each time step. In order to orthogonalize the different electronic levels, here we adopt the Gram-Schmidt orthogonalization and the Payne algorithm [30] for the choice of the Lagrange multiplier associated with the orthogonal condition. On the other hand, we treat the atomic motion by the classical Newton equation as in the original CP formalism. Such choices, however, should not be regarded as any specific feature of the mixed-basis approach; the reader should note that the mixed-basis approach is basically applicable to any other algorithms of *ab-initio* simulations mentioned above [40].

In the mixed-basis formalism,the basis $|l\rangle$ denotes either PW or AO. Suppose that we are using N_{PW} plane waves and $4N_A$ atomic orbitals accompanying the N_A atoms. Then for $l = 1, \cdots, N_{PW}$ the basis denoting the lth PW is

$$\varphi_l^{PW}(\mathbf{r}) = \langle \mathbf{r}|l\rangle = \frac{1}{\sqrt{\Omega}} e^{-i\mathbf{G}_l\cdot\mathbf{r}}. \tag{1a}$$

For $l = N_{PW} + 1, \cdots, N_{PW} + N_A$ it denotes the 1s atomic wave function (spin is neglected) centered on the $m(=l - N_{PW})$th atom, i.e.

$$\varphi_m^{1s}(\mathbf{r}) = \langle \mathbf{r}|l\rangle = \sqrt{\frac{\alpha_m^3}{\pi}}\, e^{-\alpha_m|\mathbf{r}-\mathbf{R}_m|}, \tag{1b}$$

and for $l = N_{PW} + N_A + 1, \cdots, N_{PW} + 4N_A$ it denotes one of the $2p_x$, $2p_y$, $2p_z$ atomic functions:

$$\varphi_m^{2p_x}(\mathbf{r}) = \langle \mathbf{r}|l\rangle = \sqrt{\frac{\beta_m^5}{\pi}}\,(x - X_m)\, e^{-\beta_m|\mathbf{r}-\mathbf{R}_m|}, \tag{1c}$$

$$\varphi_m^{2p_y}(\mathbf{r}) = \langle \mathbf{r}|l\rangle = \sqrt{\frac{\beta_m^5}{\pi}}\,(y - Y_m) e^{-\beta_m|\mathbf{r}-\mathbf{R}_m|}, \tag{1d}$$

$$\varphi_m^{2p_z}(\mathbf{r}) = \langle \mathbf{r}|l\rangle = \sqrt{\frac{\beta_m^5}{\pi}}\,(z - Z_m) e^{-\beta_m|\mathbf{r}-\mathbf{R}_m|}. \tag{1e}$$

Because these atomic bases are not orthogonal to the PWs, we start from the modified CP equation which guarantees the orthogonality;

$$\mu S\ddot{\Psi}_i = -(H - \Psi_i^\dagger H\Psi_i S)\Psi_i, \tag{2}$$

$$\nu_m^{1s}\ddot{\alpha}_m = -\partial E/\partial\alpha_m, \quad \nu_m^{2p}\ddot{\beta}_m = -\partial E/\partial\beta_m, \tag{3}$$

$$M_m\ddot{\mathbf{R}}_m = -\partial E/\partial\mathbf{R}_m, \tag{4}$$

where μ and ν_m denote the fictitious "masses" for electron wave functions $\Psi_i = (\langle\Psi_i|1\rangle, \langle\Psi_i|2\rangle, \langle\Psi_i|3\rangle, \cdots)^\dagger$ and other time-dependent variables α_m,

while M_m represents the real nucleus mass of the mth atom; $H(=\langle l|H|k\rangle)$ and E denote the Hamiltonian of the electrons and the total energy of the system, respectively. Hereafter we use subscripts ij for electronic levels, lk for basis functions, and mn for the atoms.

The distinguishing feature of the present equations with the mixed-basis from those of the earlier PW approaches is the presence of the overlap matrix $S(=\langle l|k\rangle)$ in Equation (2), which is due to the fact that the bases are not mutually orthogonal. Introducing the lower half triangular matrix U which satisfies $S = UU^\dagger$ and is constructed in the Choleski decomposition [38], and writing $U^\dagger\Psi_i = \Phi_i$ and $H' = U^{-1}HU^{\dagger -1}$, we finally have:

$$\mu\dot{\Phi}_i = -(H' - \Phi_i^\dagger H'\Phi_i)\Phi_i. \tag{5}$$

Once we adopt this representation, the main algorithm for updating the wave function Φ_i is the same as the original PW approach. In evaluating the charge density one needs to trace the wave functions to those in the original nondiagonal frame via the relation $\Psi_i = U^{\dagger -1}\Phi_i$. If the atomic wave function has extra parameters like exponential damping rates α_m and β_m, these parameters can also be treated as time dependent variables as in Equation (3).

The effective one-electron Hamiltonian reads

$$H = T + V, \quad T = -\frac{1}{2}\nabla^2, \tag{6a}$$

$$V(\mathbf{r}) = -\sum_m \frac{Z_m}{|\mathbf{r} - \mathbf{R}_m|} + \int d\mathbf{r}' \frac{\rho(\mathbf{r}')}{|\mathbf{r} - \mathbf{r}'|} + V^{ec}(\mathbf{r}), \tag{6b}$$

where we have used the atomic units (a.u.), $h = m_e = e = 1$. In Equation (6b), Z_m and $\mathbf{R}_m$ denote, respectively, the atomic number and the position of the mth atom, $\rho(\mathbf{r})$ is the total electron density and $V^{ec}(\mathbf{r})$ the exchange-correlation potential which is evaluated in real space under the local density approximation [32]. In our formalism, we evaluate $\rho(\mathbf{r})$ directly in real space from the expansion-coefficients determined at the previous step. We also utilize the fast Fourier transformation (FFT) for many times in the present algorithm. To calculate the electron-atom and electron-electron Coulomb potentials, i.e the first two terms in Equation (6b), it is much more efficient to evaluate their sum in the Fourier space as,

$$\bar{V}(\mathbf{G}) = 4\pi \frac{\bar{\rho}(\mathbf{G}) - \sum_m Z_m e^{-i\mathbf{G}\cdot\mathbf{R}_m}/\Omega}{G^2} \tag{7}$$

provided that the charge density $\bar{\rho}(\mathbf{G})$ in the Fourier space is known (in Equation (7) Ω denotes the volume of the unit cell). As a more elaborate matter, in order to perform a high precision integration of potential matrix elements in real space around each atom, meshes on which we evaluate the real space potential are chosen so as to contain the atomic sites at their centers. Therefore we evaluate the real space charge density $\rho_m(\mathbf{r})$ and potential $V_m(\mathbf{r})$ both centered on the mth atom for $m = 1 \sim N_A$, which is the most time-consuming part in the present computer program.

Once the potential function is determined, we then proceed to evaluate the Hamiltonian matrix elements $\langle l|H|k\rangle = \langle l|T|k\rangle + \langle l|V|k\rangle$. In the calculation

of potential matrix elements $\langle l|V|k\rangle$, there are three types of combinations: PW-PW, PW-AO, and AO-AO. For PW-PW the standard calculation in the Fourier space works well. Especially, as in the original CP method, all these PW-PW matrix elements have not to be stored in the computer-memory, because the PW-PW block is not altered after the diagonal transformation $H' = U^{-1}HU^{\dagger -1}$. On the other hand, the other combinations PW-AO and AO-AO are more easily calculated in the real space (in the small area around each atomic nucleus), since the 1s and 2p AOs presently chosen are well localized around each of nuclei sites. (For such choices of AOs, one may neglect all overlaps between different atomic orbitals located at different nuclei positions as a good approximation.) Moreover, we separate the real-space potential $V_m(\mathbf{r})$ centered on each atom into two parts; one is the spherically-symmetric and analytic part $V_m^a(r) = -6e^{-\zeta_m r}/r$ and the other is the numerical part $V_m^b(\mathbf{r}) = V_m(\mathbf{r}) - V_m^a(r)$. All the relevant integrals involving $V_m^a(r)$ are carried out analytically.

For the matrix elements of the kinetic energy $\langle k|T|k\rangle$, one has three analogous combinations; for PW-PW, PW-1s and PW-2p$_x$, i.e.

$$\langle l|T|k\rangle = \frac{1}{2}G_l^2\delta_{lk}, \quad \text{for} \quad 1 \le l, \quad k \le N_{PW} \tag{8a}$$

$$\langle l|T|N_{PW}+m\rangle = \frac{4\sqrt{\pi\alpha_m^5}}{\Omega}\frac{G_l^2}{(G_l^2+\alpha_m^2)^2}e^{-i\mathbf{G}_l\cdot\mathbf{R}_m}, \tag{8b}$$

$$\text{for} \quad 1 \le l \le N_{PW}, \quad 1 \le m \le N_A,$$

$$\langle l|T|N_{PW}+N_A+m\rangle = -i\frac{16\sqrt{\pi\beta_m^7}}{\Omega}\frac{G_l^2 G_x}{(G_l^2+\beta_m^2)^3}e^{-i\mathbf{G}_l\cdot\mathbf{R}_m}, \tag{8c}$$

$$\text{for} \quad 1 \le l \le N_{PW}, \quad 1 \le m \le N_A,$$

respectively, while, for 1s-1s and 2p$_x$-2p$_x$, one may expect the hydrogen-like analytic result, $\langle N_{PW}+n|T|N_{PW}+m\rangle = \frac{1}{2}\alpha_n^2\delta_{nm}$ and $\frac{1}{2}\beta_n^2\delta_{nm}$.

In the present formalism of the atomic dynamics, the spatial derivatives of the total energy basically read

$$\frac{\partial E}{\partial \mathbf{R}_m} = \frac{\partial\left(\sum_i \Psi_i^\dagger T\Psi_i\right)}{\partial \mathbf{R}_m} + \int \frac{\partial\rho}{\partial \mathbf{R}_m} V\,d\mathbf{r}$$

$$-\frac{\partial}{\partial \mathbf{R}_m}\sum_{n(\neq m)}\frac{Z_n Z_m}{|\mathbf{R}_n-\mathbf{R}_m|} + Z_m\int\rho(\mathbf{r})\frac{\partial}{\partial \mathbf{R}_m}\frac{d\mathbf{r}}{|\mathbf{R}_m-\mathbf{r}|}. \tag{9}$$

The first two terms represent the variational forces involving all the derivatives of AO's which depend explicitly on $\mathbf{R}_m$ via Equation (7), while the sum of the last two terms represents the Hellman-Feynman force which already exists in the original CP method using only PWs. Although the core orbitals do not affect the interatomic forces significantly, we may not neglect the first two terms (variational forces) in Equation (9) when the electronic states deviate from the BO surface. In order to keep the electronic states as close fo the BO surface as possible, our simulation

performs at each time step one extra loop for the electronic SD calculation without updating the atomic positions. We have checked that the variational force is negligibly small and that the sum of forces acting on all atoms vanishes term by term in Equation (9) with negligible error. In our simulation, we renormalize Z_m by subtracting the partial charge density from the 1s-1s part of the mth atom and use in Equation (9) the renormalized charge $\rho'(\mathbf{r})$ which is obtained from $\rho(\mathbf{r})$ also by subtracting the 1s-1s part. Finally, we evaluate the last term in Equation (9) analytically in the region near the center of the mth atom and numerically elsewhere.

6 BAND STRUCTURE CALCULATION OF ALIGNED C_{60} ON SI(100) SURFACE

There are several works concerning the calculation of electronic states of C_{60}. Saito and Oshiyama [19] calculated the band structure of a fcc C_{60} crystal for the first time, and concluded that it is a semiconductor with energy gap of 1.5 eV at X point, and alkali-metal impurity induces a shallow donor state in the gap. Hamada *et al.* [39] calculated the electronic structure of alkali-metal-doped C_{60} crystal, and obtained the Fermi surface with a peculiar shape. Although there have been considerable advances in theoretical treatments, all of these researches have been restricted to three dimensional C_{60} crystal structures, and no calculations concerning two dimensional band structure have been done before.

The recent STM study [25] indicates that the single C_{60} microcluster is tightly bound to the Si(100) surface to form a triangular c(4 × 3) structure with a charge transfer from Si dangling bonds. The *nearest neighbour* distance of C_{60} molecules in this structure is 9.6 Å which is somewhat shorter than that in the bulk fcc C_{60} (about 10.6 Å), although the C_{60} packing density is a little bit lower. They also observed black and while patterns, Figure 3, on C_{60} images which have three or four "stripes".

A mixed-basis full-potential band calculation is carried out to analyze the two dimensional band structure of the triangular-lattice C_{60} molecules. As the first step to incorporate the effect of the substrate, we model the charge transfer from Si dimers by assuming the charge neutrality with a uniform positive background. There are two distinct sites of in the c(4 × 3) structure with four or eight dangling bonds existing nearby. The possible maximum amount of the charge transfer is therefore six per one C_{60}, when we assume that every C_{60} site is geometrically equivalent and all the dangling bonds loose all of their electrons. However, somewhat less amount of charge transfer, say, for example, C_{60}^{4-}, seems to have been realized in the experiments.

In our calculation, lengths of double and single bonds between two carbons in C_{60} are fixed to be 1.40 and 1.46 Å, respectively, while two double bonds locating on opposite sides of C_{60} are fixed at the lowermost and topmost locations. We assume a rhombohedral unit cell determined experimentally [25] having a 73.74° vertex and $a = b = 9.6$ Å (la.u. = 0.52918 Å) lattice constants in the basal plane, in which the direction of dimer sequences are parallel to the shorter diagonal of the rhombohedron. With this unit cell, the two distinct C_{60} molecules are approximated to be the same in the c(4 × 3) structure. On the other hand, we use a supercell approximation to treat the vertical direction such that C_{60} repeats in a

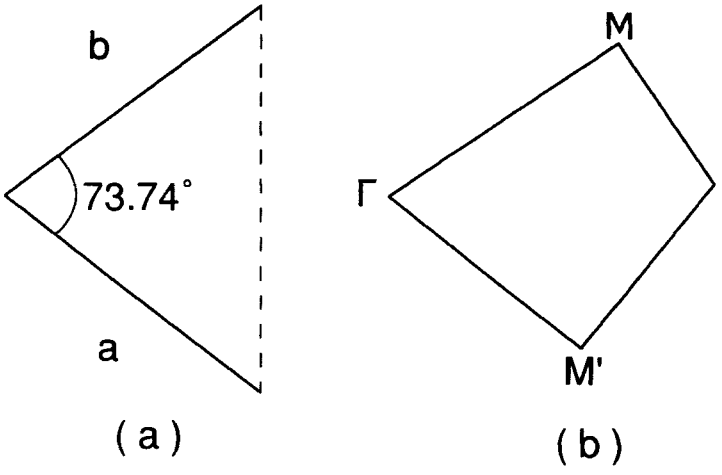

Figure 7 The unit cell and the Brillouin zone. A rhombohedral unit cell having a 73.74° vertex, the lattice constants $a = b = 9.6$ Å in the basal plane, and $c = 11.9$ Å in the perpendicular direction are used.

period of $c = 11.9$ Å, which is somewhat larger than a and b. Figure 7 shows the unit cell and the Brillouin zone.

Moreover we take the spin doublet in each level for granted. Sixty 1s atomic orbitals of C_{60} and 1865 plane waves were adopted as a basis set. The real space is divided into $64 \times 64 \times 64$ meshes, where 3.175 meshes correspond approximately to 0.529 Å. The exponential damping factors α and β for the 1s and 2p atomic wave functions are chosen as $\alpha = 1/0.106$ and $\beta = 1/0.133$ Å^{-1}, respectively. For the computation, we have used NEC SX-2N supercomputer, with which we have achieved more than 98.5% vector operation ratio.

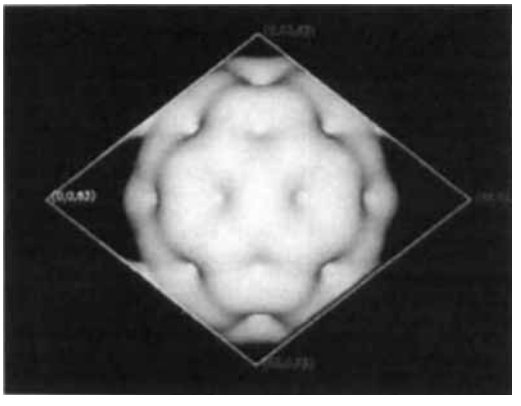

Figure 8 The spatial distribution of total charge density of C_{60}^{4-} including 1s core electrons. The charge is localized in the intermolecular region.

6.1 *Results of the* Ab-Initio *Calculations*

Here, the results of the two-dimensional band structure calculations are presented and compared with the experimental results. Figure 8 shows the spatial distribution of total charge density of C_{60}^{4-1} including 1s core electrons. It is evident that there is a net charge density around the intermolecular region, which has not been observed in the fcc C_{60}. It is confirmed that there are remarkable sharp peaks in the vicinity of C atoms, indicating that 1s core electrons are well described in our method.

Figure 9 shows the calculated band structure of the C_{60}^{4-} case. We dropped from this figure the sixty 1s bands all locating at -22 Ry. without dispertion, while we depicted the first 140 valence levels. Because of the existence of strong dispersion, there are band overlaps everywhere, and the overall feature is quite different from that obtained,for the fcc C_{60} [19], although the density of state is rather similar. This feature originates from both the existence of excess electrons transferred from the substrate, and the decrease of nearest-neighbor distance between molecules (about 1 Å smaller than that for the fcc). The lower 121 levels are completely occupied and the 122nd and 123rd levels are partly occupied, where the

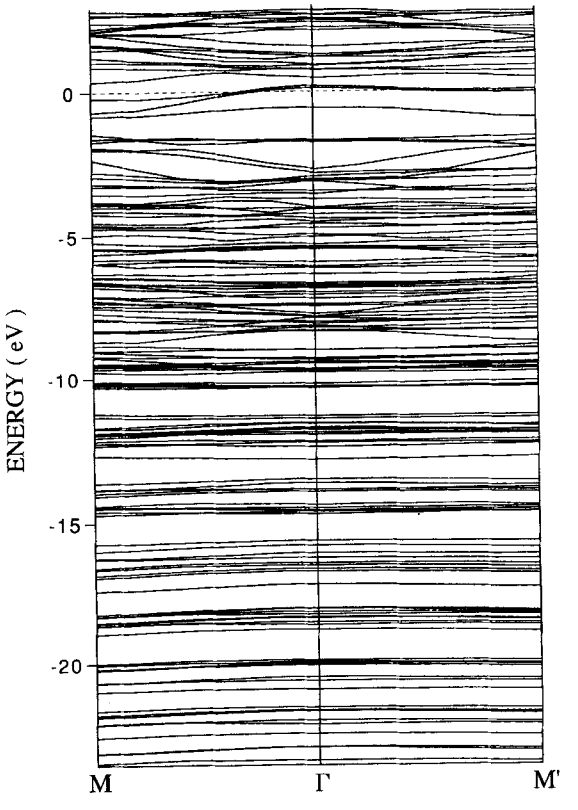

Figure 9 The calculated band structure of the C_{60}^{4-} case. Sixty 1s bands are dropped from the figure.

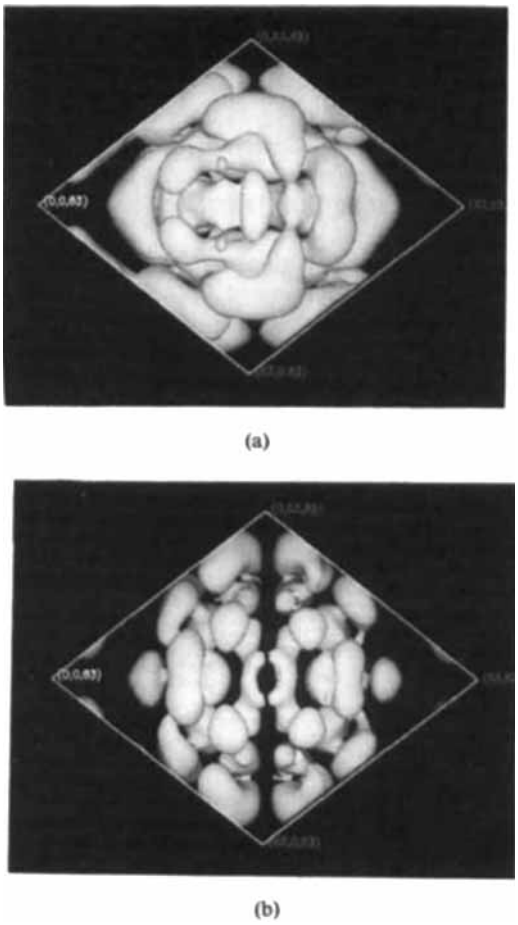

Figure 10 The spatial distribution of the partial charge density of the 122nd level (a), and the 123rd level (b) at the Γ point corresponding to the C_{60}^{4-}.

Fermi level exists (dotted horizontal line in Figure 9). The top of the 122nd band is located around the Γ point, while the bottom of the 123rd level is located at the M point which is lower in energy than the Γ point of the 122nd band. The band structure of C_{60}^{6-} was also calculated and similar result was obtained. From Figure 8 we see that the Fermi surface around Γ point is very small, indicating the existence of small number of surface free carriers.

Figure 10 shows the spatial distribution of the partial charge density of the 122nd level (a), and the 123rd level (b) at the Γ point corresponding to the C_{60}^{4-}. It is easily seen that there is a set of "stripes" in the contour map of the 123rd level parallel to the direction of the topmost double bond of C_{60}. The number of "stripes" depends not only on the direction of cutting surface of the contour but also in the band level. Three "stripes" in *xy*-plane parallel to the substrate, and four

"stripes" in *xz*- and *yz*-planes normal to the substrate are present. This feature corresponds to the STM image [25] mentioned before, and suggests good agreement between the theory and experiment. We have confirmed that the direction of stripes always coincides with the direction of topmost double bond. This result suggests that one can determine the orientation of C_{60} from the STM pattern image by identifying the direction of stripes.

We can conclude from our ab-initio calculations that the all-electron calculations using the *mixed-basis* Car-Parrinello formalism reproduce the density of states and the 1s binding energy for the carbon system correctly. The results of our band structure calculations explain accurately the experimental finding concerning the charge transfer from silicon substrate to the Buckyballs, and give a theoretical insight into the nature of the "stripes" observed on the C_{60} molecules. We can ascertain that these "stripes" must arise as a result of charge transfer.

Acknowledgements

The authors are grateful to Professors Nishina and Sakurai at our Institute for introducing us to their new STM-based experimental results. They also thank the members of the Computer Science Group at the Institute for Materials Research. We also thank IBM Japan, Kubota Computer Inc., and Japan IMSL Inc. for providing extensive computational facilities. H.R-T would like to thank the Hitachi Corp. and Tohoku University (Japan) for a Visiting Research Professorship.

References

[1] A.P. Sutton, J.B. Pethica, H. Rafii-Tabar and J.A. Nieminen, "Mechanical Properties of Metals at the Nanometer Scale", in *Electron Theory in Alloy Design*, D.G. Pettifor and A.H. Cottrell eds, Institute of Materials (London), 1992, **ch. 7**.

[2] H. Rafii-Tabar, J.B. Pethica and A.P. Sutton, "Influence of adsorbate monolayer on the nano-mechanics of tip-substrate interactions", *Proc. MRS.* **239**, (W.D. Nix *et al.* eds) Massachusetts, 313, 1992.

[3] H. Rafii-Tabar and Y. Kawazoe, "Influence of cluster size on the nano-mechanics of tip-substrate interactions", *Proc. 2nd Int. Conf. and Exn. on Computer Applications to Materials and Molecular Science and Engineering-CAMSE 92*, M. Doyama *et al.* eds, Yohokama City, Japan, 627, (1992).

[4] F.H. Stillinger and T.A. Weber, "Computer simulation of local order in condensed phases of silicon", *Phys. Rev.*, **B31**, 5262 (1985).

[5] M.W. Finnis and J.E. Sinclair, "A simple empirical N-body potential for transition metals", *Phil. Mag.*, **A50**, 45 (1984).

[6] H. Rafii-Tabar and A.P. Sutton, "Long-range Finnis-Sinclair. potentials for fcc metallic alloys", *Phil. Mag. Lett.*, **63**, 217 (1991).

[7] M.S. Daw and M.I. Baskes, "Embedded-atom method: Derivation and application to impurities, surfaces, and other defects in metals", *Phys. Rev.*, **B29**, 6443 (1984).

[8] M.I. Baskes, "Application of the Embedded-Atom method to covalent materials: A semiempirical potential for Silicon", *Phys. Rev. Lett.*, **59**, 2666 (1987).

[9] J. Tersoff, "Modelling solid-state chemistry: Interatomic potentials for multicomponent systems", *Phys. Rev.*, **B39**, 5566 (1989).

[10] D. Knuth, *The Art of Computer Programming*. (2nd edn). Addison-Wesley, Reading MA., (1973).

[11] L. Verlet, "Computer experiments on classical fluids. I. Thermodynamical properities of Lennard-Jones molecules", *Phys. Rev.*, **159**, 98 (1967) and "Computer experiments on classical fluids. II. Equilibrium correlation functions", **165**, 201 (1968).

[12] C.W. Gear, *Numerical Initial Value Problems in Ordinary Differential Equations*. Prentice-Hall, Englewood Cliffs, NJ., 1971.

[13] A.F. Hebard, M.J. Rosseinsky, R.C. Haddon, D.W. Murphy, S.H. Glarum, T.T.M. Palstra,

A.P. Rairez, and A.R. Kortan, "Superconductivity at 18 K in Potassium-doped C_{60}", *Nature*, **350**, 600 (1991).

[14] K. Tanigaki, T.T. Ebbesen, S. Saito, J. Mizuki, J.S. Tsai, Y. Kubo, and S. Kuroshima, "Superconductivity at 33 K in $Cs_xRb_yC_{60}$", *Nature*, **352**, 222 (1991).

[15] C.S. Yannoni, R.D. Johnson, G. Meijer, D.S. Bethune, and J.R. Salem, "^{13}C NMR study of the C_{60} cluster in the solid states: Molecular motion and carbon chemical shift anisotropy", *J. Phys. Chem.*, **95**, 9 (1991).

[16] P.A. Heiney, J.E. Fisher, A.R. McGhie, W.J. Ropmanow, A.M. Denenstein, J.P. Mc-Cauley Jr., A.B. Smith III, and D.E. Cox, "Orientational ordering transition in solid C_{60}", *Phys. Rev. Lett.*, **66**, 2911 (1991).

[17] Y. Guo, N. Karasawa, and W.A. Goddard III, "Prediction of fullerene packing in C_{60} and C_{70} crystals", *Nature*, **351**, 464 (1991).

[18] Q. Zhang, J.-Y. Yi, and J. Bernhole, "Structure and dynamics of solid C_{60}", *Phys. Rev. Lett.*, **66**, 2633 (1991).

[19] S. Saito and A. Oshiyama, "Cohesive mechanism and energy bands of solid C_{60}", *Phys. Rev. Lett.*, **66**, 2637 (1991).

[20] W.Y. Ching, M.-Z Zhang, Y.-N Xu, W.G. Harter, and F.T. Chan, "First-principles calculation of optical properties of C_{60} in fcc lattice", *Phys. Rev. Lett.*, **67**, 2045 (1991).

[21] L.D. Lamb, D.R. Huffman, R.K. Workman, S. Howells, T. Chen, D. Sarid and R.F. Ziolo, "Extraction and STM imaging of spherical giant Fullerenes", *Science*, **255**, 1413 (1992).

[22] R.J. Wilson, G. Meijer, D.S. Bethune, R.D. Johnson, D.D. Chambiss, M.S. de Vries, H.E. Hunziker, and H.R. Wendt, "Imaging C_{60} clusters on a surface using a scanning tunnelling microscope", *Nature*, **348**, 621 (1990).

[23] Y.Z. Li, J.C. Patrin, M. Chander, J.H. Weaver, L.P.F. Chibante, and R.E. Smalley, "Ordered overlayers of C_{60} on GaAs (110) studied with Scanning Tunnelling Microscopy", *Science*, **252**, 547 (1991).

[24] Y.Z. Li, M. Chander, J.C. Partin, J.H. Weaver, L.P.F. Chibante and R.E. Smalley, "Order and disorder in C_{60} and K_xC_{60} multilayer: Direct imaging with Scanning Tunnelling Microscopy", *Science*, **253**, 429 (1991).

[25] T. Hashizume, X.-D. Wang, Y. Nishina, H. Shinohara, Y. Saito, Y. Kuk, and T. Sakurai, "Field ion-Scanning Tunnelling Microscopy study of C_{60} on the Si(100) surface", *Jpn. J. Appl. Phys.*, **31**, L880 (1992).

[26] A. Cheng and M. Klein, "Molecular-dynamics investigation of orientational freezing in solid C_{60}", *Phys. Rev.*, **B45**, 1889 (1992).

[27] M.P. Allen and D.J. Tildesley, *Computer Simulation of Liquids*, Clarendon Press, Oxford, (1987).

[28] W. Andreoni, D. Scharf and P. Giannozzi, "Low-temperature structures of C_4 and C_{10} from the Car-Parrinello method: singlet states", *Chem. Phys. Lett.*, **173**, 449 (1990).

[29] R. Car and M. Parrinello, "Unified approach for molecular dynamics and density-functional theory", *Phys. Rev. Lett.*, **55**, 2471 (1985) & F. Buda, R. Car and M. Parrinello, "Thermal expansion of c-Si via ab-initio molecular dynamics", *Phys. Rev.*, **B41**, 1680 (1990) & G. Brocks, P.J. Kelly and R. Car, "Binding and diffuion of a-Si adatom on the Si(100) surface", *Phys. Rev. Lett.*, **66**, 1769 (1991).

[30] M.P. Teter, M.C. Payne and D.C. Allan, "Solution of Schrödinger's equation for large systems" *Phys. Rev.*, **B40**, 12255 (1989).

[31] I. Stich, R. Car, M. Parrinello, and S. Baroni, "Bonding and disorder in liquid Silicon", *Phys. Rev.*, **B39**, 4997 (1989).

[32] W. Kohn and L.J. Sham, "Self-consistent equations including exchange and correlation effects", *Phys. Rev.*, **140**, A1133 (1965) & L. Hedin and B.I. Lundqvist, "Explicit local exchange correlation potential", *J. Phys.*, **C4**, 2064 (1991).

[33] D.R. Hamann, M. Schlüter and C. Chiang, "Norm-conserving pseudopotentials", *Phys. Rev. Lett.*, **43**, 1494 (1979) & D.R. Hamann, "Generalized norm-conserving pseudopotential", *Phys. Rev.* **B40**, 2980 (1989).

[34] L. Kleinman and D.M. Bylander, "Efficacious form for model pseudopotentials", *Phys. Rev. Lett.*, **48**, 1425 (1982).

[35] X. Gonze, P. Kackell, M. Scheffier, "Ghost states for separable, norm-conserving, ab initio pseudopotentials", *Phys. Rev.*, **B41**, 12264 (1990).

[36] J.P. Perdew, in *Local Density Approximations in Quantum Chemistry and Solid State Physics*, edited by J.P. Dahl and J. Avery (Plenum Press, New York, 1984).

[37] C. Friedli and N.W. Ashcroft, "Combined representation method for use in band-structure calculation: Applicaton to highly compressed hydrogen", *Phys. Rev.*, **B16**, 662 (1977).

[38] S.G. Louie, K.-M. Ho and M.L. Cohen, "Self-consistent mixed-basis approach to the electronic structure of solids", *Phys. Rev.*, **B19**, 1774 (1979).

[39] N. Hamada, S. Saito, Y. Miyamoto, A. Oshiyama, "Fermi surfaces of alkali-metal-doped C_{60} solid", *Jpn. J. Appl. Phys.*, **30**, L2036 (1992).

[40] H. Kamiyama, K. Ohno, Y. Maruyama, and Y. Kawazoe, "*Ab-initio* molecular dynamics simulation of C_{60}", *Proc. Int. Symp. on the Physics and Chemsitry of Finite Systems*, edited by P. Jena et al, Kluwer Academic Publishers, **Vol. II**, 1335 (1992).

[41] H. Kamiyama, K. Ohno, Y. Maruyama, Y. Kawazoe, Y. Nishina, "Ab-initio Molecular Dynamics Simulation of Monolayer C_{60} Thin Film on Silicon (100) Surface", *Z. Phys. D*, in press.